Gravity wave Behavior in Lower Stratosphere during Tropical Cyclones over the Bay of Bengal

Gargi Rakshit[1], Soumyajyoti Jana[1], and Animesh Maitra[1]
[1]Institute of Radio Physics and Electronics, University of Calcutta,
92, A. P. C. Road, Kolkata-700009, India
Corresponding author: Animesh Maitra (animesh.maitra@gmail.com)

Key Points:

- Gravity wave potential energy enhancement occurs in the lower stratosphere (19-26 km) prior to tropical cyclones over the storm paths.
- The power spectral density of gravity waves reveals that the vertical wavelengths of 2-2.4 km carry most of the energy within 19 to 26 km.
- Higher gravity wave potential energy corresponds to lower outgoing long wave radiation (OLR) value.

This article has been accepted for publication and undergone full peer review but has not been through the copyediting, typesetting, pagination and proofreading process which may lead to differences between this version and the Version of Record. Please cite this article as doi: 10.1029/2018RS006614

Abstract

Gravity waves associated with tropical cyclones over the Bay of Bengal have been studied using COSMIC GPS radio occultation measurements. The sources of gravity waves are located well below the tropopause where the intensity of a tropical cyclone (TC) is high. The gravity wave potential energy between 19 to 26 km shows an enhancement in the lower stratosphere (LS) during the cyclone. Intense convection associated with TC is characterized by low outgoing longwave radiation (OLR) values. The present study shows an increase in potential energy in the lower stratosphere over a storm path before the actual occurrence of cyclones. The power spectral density of gravity waves shows that the vertical wavelengths in the range 2-2.4 km carry the maximum energy in the lower stratosphere over the cyclone path.

1. Introduction

Atmospheric gravity waves (GW) are generated as the interplay of earth's gravity and buoyancy force restoring any vertical movement of the air parcel in the atmosphere (Tsuda, 2014). Gravity waves can originate from various meteorological disturbances, deep convection like a tropical cyclone (Alexander & Holton, 1997; Alexander et al., 1995) and from different orographic effects (Ratnam et al., 2004; Tsuda, 2014). These waves transport energy and momentum from lower to upper atmosphere (Das et al., 2014). Previous studies revealed that the origins of gravity wave are located in the lower troposphere where the cyclone is intense (Tsuda, 2014; Ratnam et al., 2016). As gravity waves generated in the lower troposphere propagate to the upper atmosphere, they influence the zonal and the meridional wind pattern and change the atmospheric general circulation (Holton, 1983; Alexander et al., 2008). Tropical convection generates high frequency gravity waves, having significant role in changing the middle atmospheric general circulation (Dutta et al., 2009). Statistical analysis of the characteristics of wave number spectra of gravity waves in the tropical troposphere has been carried out using Mesosphere-Stratosphere-Troposphere (MST) radar observations over Gadanki, India (Babu et al., 2008). Characteristics of high frequency GWs and inertia gravity waves have investigated from high resolution radiosonde observations over a tropical location Gadanki (Leena et al., 2012a, 2012b).The gravity wave energy produced by a TC is larger than that produced by local convection (Chane Ming et al., 2010). The importance of deep convection like intense cyclone in the tropics as the source of GW was highlighted by previous findings where orographic disturbances were negligible (Chun et al., 2001; Fritts & Rastogi, 1985). Tropical cyclone (TC) plays an important role in the exchange processes between upper troposphere (UT) and lower stratosphere (LS) (Ravindra Babu et al., 2015; Das et al., 2016), and in changing the tropopause structure (Ratnam et al., 2016). Tropical cyclone leads to the transport of water vapour from troposphere to lower stratosphere and ozone from lower stratosphere to upper troposphere (Ray & Rosenlof, 2007). The studies of Piani et al. (2000) and Fritts et al. (2003) emphasized the significance of cumulus convection during tropical cyclones. This shows the importance of the study of GW activities in lower stratosphere as an evidence of stratosphere troposphere exchange processes. Ibrahim et al. (2010) showed that GW energy in the LS can be utilized as an index to investigate TC activities.

The very high frequency (VHF) radar, MST radar and lidar observations have enabled GW studies with good temporal and spatial resolution (Wilson et al., 1991; Chang et al., 1997; Worthington & Thomas, 1996; Vincent & Eckermann, 1990; Rastogi et al., 1996; Das et al., 2012). But the ground based instruments failed to observe GW activities over the ocean which is the source of cyclones. GPS radio occultation measurements facilitate the study of

GW over the oceans. The Bay of Bengal (BoB) is the genesis of 10-12% of the total yearly TCs over the globe (Neuman, 1993; Ibrahim et al., 2010) with an annual average of five cyclones having unpredictable intensity and track (Raghavan & Sen Sarma, 2000; Rao et al., 2001; Bindu et al., 2016). Geller & Gong (2010) provided the climatology of kinetic energy and potential energy in relation to monthly and latitudinal variations at different frequencies of GW.

Seasonal analysis focussed that large amount of potential energy are generated at low latitudes below 25 km height in all seasons (Tsuda et al., 2000, 2004; Vincent & Alexander, 2000). Chane Ming et al. (2002) found the existence of large amplitude gravity waves in UT/LS during intense tropical cyclone 'Hudah' over the Tromelin Island. GW signature of cyclones Dina and Faxai have been investigated using GPS windsonde profiles (Chane Ming et al., 2010). Numerical models like Weather Research and Forecast (WRF) have been used to predict the cyclone path of Phailin (Bindu et al., 2016). The study of the enhancement of gravity waves before the appearance of cyclones in the lower stratosphere has not yet been reported. The present study has a focus on the gravity wave energy activities before, during and after the dissipating stage of the cyclonic storm using Constellation Observing System for Meteorology, Ionosphere and Climate (COSMIC) GPS Radio Occultation (RO) data. Satellite observations can provide global coverage to investigate the quantitative picture of GW activities (Wu & water, 1996; Mc Landress et al., 2000). However, compared to the ground based measurements, the temporal resolution of satellite based observation is not as good. An enhancement of potential energy (E_p) associated with the storm is noticed in the lower stratosphere (19 to 26 km). The spatial evolution of gravity wave characteristics in the lower stratosphere in terms of potential energy and spectral analysis has been studied for five tropical cyclones namely; Sidr, Aila, Giri, Nargis, and Phailin. Five representative cases of intense cyclone with peak wind intensity greater than 100 km/hr occurred over Bay of Bengal in different years have been considered in the present study. The paper is organised into five sections. Section 2 describes the data and methodology. Section 3 illustrates about the variation of gravity wave potential energy and dominant vertical wavelengths before, during and after the five tropical cyclones over cyclone affected region. Discussions of the results are given in Section 4, and, finally, concluding remarks are included in Section 5.

2. Data and Methodology

The potential energy estimation and spectral analysis have been obtained using the temperature data from COSMIC GPS RO. COSMIC satellite data are obtained from COSMIC Data Analysis and Archive Center (CDAAC). The COSMIC reprocessed data (available from May 2006 – May 2014) have been used for the present study. GPS occultation is used for the retrieval of the refractivity profile from lower heights of the atmosphere (above 10 km) up to an altitude of 40 km (Tsuda, 2017). From the refractivity profile, 'dry temperature' profile is derived by neglecting the water vapour content. In the present study dry temperature profiles from the COSMIC RO data are used (Alexander et al., 2008).

The temperature data obtained from GPS RO offer good altitude resolution (Alexander et al., 2009). Considering all the available occultations, COSMIC RO data are taken over each grid size of 8° x 8° for the latitude range of 4-45° N and longitude range of 65-100° E. A sudden temperature change near the tropopause contaminates potential energy (E_p) estimation (Hei et al., 2008). The height range from 19 to 26 km is considered during the months of the TCs, for estimating the potential energy in lower stratosphere. As the primary objective is to estimate the potential energy during tropical cyclones, the monthly mean of temperature profiles of each grid is calculated. The monthly mean temperature profiles are

low pass filtered using 4 km running average along the height. The filtered profile is taken as the background temperature profile ($\bar{T}$) of the respective grid (Hei et al., 2008; Tsuda et al. 2009). To calculate the perturbation profiles (T'), the individual temperature profile of the respective grid is subtracted from the background temperature ($\bar{T}$) within that grid. A linear fit is subtracted from the perturbation profile to remove any linear trend along the height. Also, a half cosine windowing function is applied to eliminate the edge effect in the profile. This is equivalent to multiplying a cosine function with the data at the height ranges 19-19.7 km and 25.3-26 km. Now FFT is applied to extract the vertical wavelength present in the perturbation profile (Hei et al., 2008; Tsuda et al. 2009). The wave number 0 and 1 (7 km) are removed and then inverse FFT is done to reproduce the perturbation profile (T') considering the wave numbers greater than 1. Since we have considered the height range 7 km (19-26 km) in the lower stratosphere, wavenumber 1 corresponds to a wavelength of 7 km. Hence, Finally, the temperature perturbation profiles (T') are obtained having vertical wavelengths less than 7 km (Hei et al., 2008; Tsuda et al. 2009).

Figure 1 (a) shows an individual temperature profile and the mean profile in a cyclone affected grid during the tropical cyclone Sidr. The perturbation profile for the location (12.44°N, 89.73° E) on 11 November 2007, obtained using the above mentioned procedure, is plotted in Figure 1 (b). The potential energy is calculated from the perturbed profile using the following relation (Tsuda et al., 2004, 2009; Vincent & Alexander, 2000,).

$$E_p = \frac{1}{2}\left[\left(\frac{g}{N}\right)^2 \overline{\left(\frac{T'}{\bar{T}}\right)^2}\right] \quad (1)$$

$\bar{T}$ and T' represent the mean and perturbed atmospheric temperature respectively. N and g are Brunt–Väisälä frequency and acceleration due to gravity respectively (Tsuda et al., 2004). Brunt–Väisälä frequency is calculated from the relation (2) (Stull 1995).

$$N = \left(\frac{g}{\theta}\frac{\partial\theta}{\partial z}\right)^{1/2} \quad (2)$$

θ is the potential temperature and $\frac{\partial\theta}{\partial z}$ is the vertical gradient of potential temperature. This methodology has been followed for the five TCs studied in this paper.

The total number of occultation events which are found within 4°-45° E and 65°-100° E for different storms have been included in Table 1. In the estimation of the gravity wave potential energy (E_p) values over the selected region, the temperature profile over 8° x 8° grid area is considered and then averaged by using a sliding window width of 2° x 2° in latitude and longitude. The total and average number of occultation events over the said region and each grid of the cyclone are given in the Table 1. The number of occultations can be retrieved from the CDAAC database website (https://cdaac-www.cosmic.ucar.edu/cdaac/DBif/cdaac_highlevel.cgi). The table shows that sufficient numbers of occultations are available to have a meaningful estimation of GW energy. It may be mentioned that at least 50 occultations in each grid (8° x 8°) are available for obtaining monthly average of temperature profiles ($\bar{T}$) as background information.

Outgoing long wave radiation (OLR) data are obtained from the Advanced Very High Resolution Radiometer (AVHRR) instrument aboard the National Oceanic and Atmospheric Administration (NOAA) polar orbiting spacecraft. The ascending and descending swath data have been spatially and temporarily interpolated onto grids of resolution 2.5° x 2.5° for using the OLR data during the five tropical cyclones considered in the study. Strong convective phenomena can be evidenced by low OLR observations. Five tropical cyclones namely; Sidr, Aila, Giri, Nargis and Phailin have been studied in the present paper. Information about the storm track have been obtained from the NOAA archive (http://rammb.cira.colostate.edu/products/tc_realtime/index.asp).

3 Results

The present study deals with the gravity wave (GW) characteristics and associated phenomena in the lower stratosphere (19-26 km) during the five tropical cyclones over the cyclone affected region occurring over the Bay of Bengal. The gravity wave characteristics of the TCs namely Sidr, Aila, Giri, Nargis and Phailin cyclones are discussed in the following sections.

3.1. E_p variation over the Bay of Bengal during the tropical cyclones

3.1.1 Sidr

Cyclone Sidr was one of the most intense cyclones on record to make its land fall over Bangladesh. This cyclone, a Category 4 storm (according to Saffir-Simpson scale), originated in the centre of Bay of Bengal on 9 November 2007, arrived at the south-western coast of Bangladesh on 15 November 2007. It intensified to turn into a very severe cyclonic storm while moving to the north-east direction on 11 November 2007, the peak wind speed reaching up to 250 km/h. The path followed by Sidr is depicted in Figure 2(a) by filled circles superimposed on the outgoing long wave radiation plot during the cyclone period (11-16 November 2007). It shows that the cyclone affected region is characterised by low OLR value (less than 180 W/m^2) indicating deep convection in the region.

The average potential energy of gravity wave in the lower stratosphere (19-26 km) is calculated before (3-10 November 2007), during (11-16 November 2007) and after (22-29 November 2007) the cyclone using COSMIC RO temperature data. It is observed from the contour plot of potential energy that there is an increase in E_p (1.94 J/kg) along the storm track before the cyclone (Figure 2 (b)) which spread over the adjoining region during the cyclone period (Figure 2 (c)) with average E_p of 2.34 J/kg. The energy dissipated after the cyclone is over (Figure 2 (d)).

3.1.2. Nargis

Nargis was the first named storm of the 2008 North Indian Ocean Cyclone Season, which originated in 27 April 2008 in the central Bay of Bengal and moved to north-eastward as shown in Figure 3 (a) by filled circles on the OLR plot. The highest wind speed was 215 km/h during the cyclone. After passing over Myanmar and Rangoon the storm dissipated near the border region of Myanmar and Thailand (Figure 3(a)). Nargis was marked Category 4, an extremely severe cyclonic storm. The average OLR value during 27 April-3 May 2008 was low (below 170 W/m^2) over the cyclone affected region indicating strong convective

activities. This played an active role in generating gravity waves and caused an enhancement of E_p over the cyclone affected region as shown in Figure 3 (c).

Three separate time spans namely, before the storm (18-26 April 2008), during the storm (27 April-03 May 2008) and after the storm Nargis (8-16 May 2008), have been considered to estimate E_p. The potential energy value shows an increase over the storm path (average E_p value of 2.32 J/kg) before the cyclone (Figure 3(b)). During the storm the energy increased to higher value (3.10 J/kg) (Figure 3(c)) and after the storm the energy gradually dissipated (1.16 J/kg) as shown in Figure 3(d). High E_p values in lower stratosphere over the Bay of Bengal (Figure 3(c)) show good agreement with low OLR values during the cyclone.

3.1.3. Aila

Aila evolved from a tropical disturbance in the central Bay of Bengal. The disturbance slowly developed over a period of 2 to 3 days and became a tropical storm in the early hours of 23 May 2009, as it moved northward towards West Bengal in India. Joint Typhoon Warning Center reported that the tropical disturbance moved over a distance of 950 km having the landfall at the south of the city of Kolkata in India. Filled circles on the average OLR plot in Figure 4 (a) shows the path of the cyclone over the Bay of Bengal and adjacent region of West Bengal where Aila made its landfall. Aila, was identified as Category 1 cyclone, the maximum wind speed reaching up to 120 km/h. Figure 4 (a) shows that Aila affected region is characterised by very low OLR value (below 150 W/m^2) during 22-27 May 2009.

The contour plots of E_p, before (15-21 May 2009), during (22-27 May 2009) and after (2-10 June, 2009) the tropical cyclone Aila are shown in Figure 4 (b), (c) and (d) respectively. It is observed that there is a large increase of E_p before and during the cyclone period over Bay of Bengal and adjacent areas of West Bengal.

3.1.4. Giri

Very Severe Cyclonic Storm Giri originated on 19 October 2010 over the Bay of Bengal and intensified while moving towards the north-eastern part of the Bay of Bengal. The cyclone was identified as Category 4 having the highest wind speed of 250 km/h. Giri had its landfall in Myanmar on 22 October 2010 and after which it gradually weakened. The path of Giri is shown in Figure 5(a) depicted by filled circles superimposed on the OLR contour plot. The deep convection during the cyclone Giri was characterised by low OLR values (below 170 W/m^2) over the cyclone affected region (Figure 5(a)).

The evolution of potential energy before (15-19 October, 2010), during (20-23 October 2010) and after (28 October-4 November 2010) Giri are shown in Figure 5 (b) (c), and (d) respectively. Like other cyclones, the enhancement of E_p before cyclone over the cyclone path is also noticed (Figure 5(b)). The potential energy remained high during the cyclone days (Figure 5(c)) which gradually dissipated few days after the cyclone (Figure 5(d)).

3.1.5. Phailin

According to India Meteorological Department (IMD), Phailin is an extreme intense tropical cyclone making a landfall in Odisha, India. The cyclone was identified as a Category 5 according to Saffir-Simpson scale. Developing from a depression in the Gulf of Thailand on 4 October 2013, it moved westward to pass over the Andaman and Nicobar

Islands in the Bay of Bengal and made its landfall at Gopalpur in Odisha, India, on 12 October 2013. The path of Phailin is shown in Figure 6(a) marked by filled circles. The highest wind speed during Phailin was 260 km/h. The average OLR data over the cyclone affected region was below 180 W/m^2, during 4-14 October 2013 as shown in Figure 6(a), indicating strong convective activities over this region.

It is observed that high value of E_p (2.37 J/kg) prevailed along the path of the cyclone even before the actual occurrence of Phailin (Figure 6(b)). Figure 6(c) again shows the prominent enhancement of E_p during Phailin (3.01 J/kg), and the decay of E_p (1.48 J/kg) after the dissipation of cyclone is evident from Figure 6(d).

3.2 Dominant vertical wavelengths of gravity waves

To find out the dominant vertical wavelength, power spectral density has been obtained by Welch method (Welch, 1967; Barbe et al., 2010; Zhang et al., 2009) from the temperature perturbation profiles over 8° x 8° grid as described in the methodology section. The dominant vertical wavelengths responsible for carrying energy to the lower stratosphere over the cyclone affected grids have been derived from the power spectrum.

Figure 7 shows the power spectral density before, during and after the five tropical cyclones discussed earlier. The power spectral density shows peak around 2-2.4 km vertical wavelength. However, the magnitude of the peak density is the highest during the storm. It is seen that the wavelength around 2.4 km is dominant for the propagation of gravity wave energy during the storm. The features of gravity waves during the five cyclones are given in Table 2.

4 Discussions

Depending on the availability of the number of occultations over the cyclone affected grids the average potential energy of gravity wave has been estimated in the lower stratosphere for the five tropical cyclones of different intensities. Table 2 shows that the average potential energy over the cyclone affected region shows no significant variation with the cyclone intensity which is consistent with the findings of Ibrahim et al. (2010).

In the present study, the potential energy has been found to increase in LS (19-26 km) during TCs. This is consistent with the findings of Chane Ming et al. (2002, 2010) which showed an increase of total GW energy density during tropical cyclones. Previous studies showed that a significant part of total energy propagates in the upward direction in the lower stratospheric region during cyclones (Pramitha et al., 2016). One of the important present findings is that an increase of E_p is also noticed in the lower stratosphere prior to the actual occurrence of TC. In the tropical region the average tropopause altitude is about 17 km which increases during tropical cyclones (Reid & Gage 1985; Gettelman et al., 2002). The maximum tropopause height is found to be about 18.5 km during the five tropical cyclones over the cyclone affected region considered. In order to ensure that the enhancement in temperature fluctuations is due to gravity wave and not because of the presence of tropopause, 19 km is chosen as the lowest height. It may be noted that De la Tore et al. (2006) and Tsuda et al. (2009) also set the minimum altitude for the gravity wave analysis at 19 km after considering the tropopause height variation.

Outgoing long wave radiation (OLR) values are used as proxy for convection in tropical and subtropical regions. The cyclone affected regions for the five tropical cyclones over the Bay of Bengal are found to be characterised by low OLR values during the cyclone

days (Table 2). This is again consistent with the previous findings where large values of GW energy are associated with low OLR values during TCs and deep convection (Ibrahim et al., 2010; Ratnam et al., 2008). However the values of OLR during the TCs showed no dependence on the intensity of the tropical cyclones.

Recent studies have highlighted that the average GW energy attains large values during TCs compared to that during local convection (Ibrahim et al., 2010). In the present study, GW potential energy is found to be higher during the cyclone days compared to that before and after the cyclone period. GW potential energy has been estimated from the perturbations in temperature profiles of GPS RO which do not give total energy estimate because of the absence of the information on horizontal wind. However, it is shown by Tsuda et al. (2000) and Ratnam et al. (2004) that the ratio of kinetic to potential energy is constant according to the linear theory of gravity wave and the potential energy can be indicative of the total energy.

Previous studies reported that gravity waves of dominant vertical wavelengths of 1.5 to 3 km were observed over the cyclone affected region of Tromelin Island during the passage of cyclone Hudah (Chane Ming et al., 2002). The characteristics of low frequency GW in UT/LS is related to the temporal and spatial extent of the cyclone (Chane Ming et al., 2010). Chane Ming et al. (2014) showed that low frequency gravity waves of periods of 4.6-13 h and vertical wavelengths of 0.7-3 km occurred during TC Ivan. Vertical wavelengths ranging from 0.8 to about 3 km prevailed during the cyclones Dina and Faxai in the LS over the affected region (Chane Ming et al., 2010). In the present study, the dominant vertical wavelength of gravity wave during five TCs has been found to be around 2.4 km. However, the magnitude of the spectral peak does not depend on the cyclone intensity.

5 Conclusions

The gravity wave activities associated with tropical cyclones over the Bay of Bengal have been investigated using GPS radio occultation data. The potential energy of gravity waves is estimated before, during and after the tropical cyclones. Intense convective activities associated with TC are characterized by very low OLR values which are well correlated with high potential energy distribution in the lower stratosphere. The tropical cyclones which excite atmospheric gravity waves that carry energy from troposphere to lower stratosphere. Significant increase in E_p in lower stratosphere over the storm path is noticed before the arrival of tropical cyclones. This has been observed for all the five cyclones considered in this study. A study of the power spectral density of gravity waves shows that the vertical wavelength in the range 2-2.4 km is the dominant wavelength responsible for carrying energy to the lower stratosphere over the cyclone path.

Acknowledgments

This work has been supported by the grants under the projects: (i) "Council of Scientific and Industrial Research (CSIR), HRDG (File No: 09/028(1040)/2 018-EMR-I)", (ii) "Studies on aerosol environment at Kolkata located near the land-ocean boundary as a part of ARFI network under ISRO- GBP" (Grant No: SPL:GBP:ARFI:37), and (iii) "UGC Basic Science Research Faculty Fellowship" (No.F.18-1/2011(BSR)). COSMIC Data have been acquired from COSMIC Data Analysis and Archive Centre (CDAAC) and OLR and cyclone track data are obtained from NOAA data archive. The authors are thankful to the reviewers for their helpful suggestions in improving the quality of the paper.

References

Alexander, M. J., & Holton, J. R. (1997). A model study of zonal forcing in the equatorial stratosphere by convectively induced gravity waves. *Journal of the Atmospheric Sciences*, *54*(3), 408-419.

Alexander, M. J., Holton, J. R., & Durran, D. R. (1995). The gravity wave response above deep convection in a squall line simulation. *Journal of the Atmospheric Sciences*, *52*(12), 2212-2226.

Alexander, S. P., Klekociuk, A. R., & Tsuda, T. (2009). Gravity wave and orographic wave activity observed around the Antarctic and Arctic stratospheric vortices by the COSMIC GPS-RO satellite constellation. *Journal of Geophysical Research: Atmospheres*, *114*(D17). D17103.

Alexander, S. P., Tsuda, T., & Kawatani, Y. (2008). COSMIC GPS Observations of Northern Hemisphere winter stratospheric gravity waves and comparisons with an atmospheric general circulation model. *Geophysical Research Letters*, *35*(10), L10808.

Babu, A. N., Kumar, K. K., Kumar, G. K., Ratnam, M. V., Rao, S. V. B., & Rao, D. N. (2008). Long-term MST radar observations of vertical wave number spectra of gravity waves in the tropical troposphere over Gadanki (13.5◦ N, 79.2◦ E): comparison with model spectra. *Annales Geophysicae*, *26*, 1671-1680.

Bindu, H. H., Ratnam, M. V., Yesubabu, V., Rao, T. N., Kesarkar, A., & Naidu, C. V. (2016). Characteristics of cyclone generated gravity waves observed using assimilated WRF model simulations over Bay of Bengal. *Atmospheric Research*, *180*, 178-188.

Barbe, K., Pintelon, R., & Schoukens, J. (2010). Welch method revisited: nonparametric power spectrum estimation via circular overlap. *IEEE Transactions on signal processing*. *58*(2): 553-565.

Chane-Ming, F., Chen, Z., & Roux, F. (2010). Analysis of gravity-waves produced by intense tropical cyclones. *Annales Geophysicae, 28*(2), 531-547.

Chane Ming, F., Ibrahim, C., Barthe, C., Jolivet, S., Keckhut, P., Liou, Y. A., & Kuleshov, Y. (2014). Observation and a numerical study of gravity waves during tropical cyclone Ivan (2008). *Atmospheric Chemistry and Physics*, *14*(2), 641-658.

Chane-Ming, F., Roff, G., Robert, L., & Leveau, J. (2002). Gravity wave characteristics over Tromelin Island during the passage of cyclone Hudah. *Geophysical Research Letters*, *29*(6). 18-1-18-4.

Chang, J. L., Avery, S. K., Riddle, A. C., Palo, S. E., & Gage, K. S. (1997). First results of tropospheric gravity wave momentum flux measurements over Christmas Island. *Radio Science*, *32*(2), 727-748.

Chun, H. Y., Song, M. D., Kim, J. W., & Baik, J. J. (2001). Effects of gravity wave drag induced by cumulus convection on the atmospheric general circulation. *Journal of the Atmospheric Sciences*, *58*(3), 302-319.

Das, S. S., Kumar, K. K., Uma, K. N., Ratnam, M. V., Patra, A. K. et al. (2014). Modulation of thermal structure in the upper troposphere and lower stratosphere (UTLS) region by inertia gravity waves: A case study inferred from simultaneous MST radar and GPS sonde observations. *Indian Journal of Radio and Space Physics, 43*(1), 11-23.

Das, S. S., Ratnam, M. V., Uma, K. N., Subrahmanyam, K. V., Girach, I. A. et al. (2016). Influence of tropical cyclones on tropospheric ozone: possible implications. *Atmospheric Chemistry and Physics*, *16*(8), 4837-4847.

Das, S. S., Uma, K. N., & Das, S. K. (2012). MST radar observations of short-period gravity wave during overhead tropical cyclone. *Radio Science*, *47*(2), RS2019.

De la Torre, A., Schmidt, T., & Wickert, J. (2006). A global analysis of wave potential energy in the lower stratosphere derived from 5 years of GPS radio occultation data with CHAMP. *Geophysical Research Letters*, *33*(24), L248009.

Dutta, G., Kumar, A., Vinay Kumar, P., Venkat Ratnam, M., Chandrashekar, M. et al. (2009). Characteristics of high-frequency gravity waves generated by tropical deep convection: Case studies. *Journal of Geophysical Research: Atmospheres*, *114*(D18), D18109.

Fritts, D. C., & Alexander, M. J. (2003). Gravity wave dynamics and effects in the middle atmosphere. *Reviews of Geophysics*, *41*(1), 3-1-3-64.

Fritts, D. C., & Rastogi, P. K. (1985). Convective and dynamical instabilities due to gravity wave motions in the lower and middle atmosphere: Theory and observations. *Radio Science*, *20*(6), 1247-1277.

Gettelman, A., Salby, M. L., & Sassi, F. (2002). Distribution and influence of convection in the tropical tropopause region. *Journal of Geophysical Research: Atmospheres*, *107*(D10), ACL-6-1-ACL-6-12.

Geller, M. A., & Gong, J. (2010). Gravity wave kinetic, potential, and vertical fluctuation energies as indicators of different frequency gravity waves. *Journal of Geophysical Research: Atmospheres*, *115*(D11), D11111.

Hei, H., Tsuda, T., & Hirooka, T. (2008). Characteristics of atmospheric gravity wave activity in the polar regions revealed by GPS radio occultation data with CHAMP. *Journal of Geophysical Research: Atmospheres*, *113*(D4), D04107.

Holton, J. R. (1983). The influence of gravity wave breaking on the general circulation of the middle atmosphere. *Journal of the Atmospheric Sciences*, *40*(10), 2497-2507.

Ibrahim, C., Chane-Ming, F., Barthe, C., & Kuleshov, Y. (2010). Diagnosis of tropical cyclone activity through gravity wave energy density in the southwest Indian Ocean. *Geophysical Research Letters*, *37*(9), L09807.

Leena, P. P., Ratnam, M. V., & Murthy, B. K. (2012). Inertia gravity wave characteristics and associated fluxes observed using five years of radiosonde measurements over a tropical station. *Journal of Atmospheric and Solar-Terrestrial Physics*, *84*, 37-44.

Leena, P. P., Ratnam, M. V., Murthy, B. K., & Rao, S. V. B. (2012). Detection of high frequency gravity waves using high resolution radiosonde observations. *Journal of Atmospheric and Solar-Terrestrial Physics*, *77*, 254-259.

McLandress, C., Alexander, M. J., & Wu, D. L. (2000). Microwave Limb Sounder observations of gravity waves in the stratosphere: A climatology and interpretation. *Journal of Geophysical Research: Atmospheres*, *105*(D9), 11947-11967.

Neumann, C. (1993). Global overview in Global Guide to Tropical Cyclone Forecasting, WMO Trop. Cyclone Program Rep. TCP-31, chap. 1, pp. 43, World Meteorol. Organ., Geneva, Switzerland.

Piani, C., Durran, D., Alexander, M. J., & Holton, J. R. (2000). A numerical study of three-dimensional gravity waves triggered by deep tropical convection and their role in the dynamics of the QBO. *Journal of the Atmospheric Sciences*, *57*(22), 3689-3702.

Pramitha, M., Ratnam, M. V., Leena, P. P., Murthy, B. K., & Rao, S. V. B. (2016). Identification of inertia gravity wave sources observed in the troposphere and the lower stratosphere over a tropical station Gadanki. *Atmospheric Research*, *176*, 202-211.

Raghavan, S., & Sen Sarma, A. K. (2000). Tropical cyclone impacts in India and neighbourhood. *Storms*, *1*, 339-356.

Rao, D. B., Naidu, C. V., & Rao, B. S. (2001). Trends and fluctuations of the cyclonic systems over North Indian Ocean. *Mausam*, *52*(1), 37-46.

Rastogi, P. K., Kudeki, E., & Sürücü, F. (1996). Distortion of gravity wave spectra of horizontal winds measured in atmospheric radar experiments. *Radio Science*, *31*(1), 105-118.

Ravindra Babu, S., Venkat Ratnam, M., Basha, G., Krishnamurthy, B. V., & Venkateswararao, B. (2015). Effect of tropical cyclones on the tropical tropopause parameters observed using COSMIC GPS RO data. *Atmospheric Chemistry and Physics*, *15*(18), 10239-10249.

Ray, E. A., & Rosenlof, K. H. (2007). Hydration of the upper troposphere by tropical cyclones. *Journal of Geophysical Research: Atmospheres*, *112*(D12).

Reid, G. C., & Gage, K. S. (1985). Interannual variations in the height of the tropical tropopause. *Journal of Geophysical Research: Atmospheres*, *90*(D3), 5629-5635.

Stull, R. B. (1995). *Meteorology Today for Scientists and Engineers: A Technical Companion Book to Meteorology Today by C. Donald Ahrens*. West Publishing Company.

Tsuda, T. (2014). Characteristics of atmospheric gravity waves observed using the MU (Middle and Upper atmosphere) radar and GPS (Global Positioning System) radio occultation. *Proceedings of the Japan Academy, Series B*, *90*(1), 12-27.

Tsuda, T. (2017). Comparison of three retrievals of COSMIC GPS radio occultation results in the tropical upper troposphere and lower stratosphere. *Earth, Planets and Space*, *69*(1), 125.

Tsuda, T., Nishida, M., Rocken, C., & Ware, R. H. (2000). A global morphology of gravity wave activity in the stratosphere revealed by the GPS occultation data (GPS/MET). *Journal of Geophysical Research: Atmospheres*, *105*(D6), 7257-7273.

Tsuda, T., Ratnam, M. V., Alexander, S. P., Kozu, T., & Takayabu, Y. (2009). Temporal and spatial distributions of atmospheric wave energy in the equatorial stratosphere revealed by GPS radio occultation temperature data obtained with the CHAMP satellite during 2001–2006. *Earth, Planets and Space*, *61*(4), 525-533.

Tsuda, T., Ratnam, M. V., May, P. T., Alexander, M. J., Vincent, R. A., & MacKinnon, A. (2004). Characteristics of gravity waves with short vertical wavelengths observed with radiosonde and GPS occultation during DAWEX (Darwin Area Wave Experiment). *Journal of Geophysical Research: Atmospheres*, *109*(D20), D20S03.

Venkat Ratnam, M., Narendra Babu, A., Jagannadha Rao, V. V. M., Vijaya Bhaskar Rao, S., & Narayana Rao, D. (2008). MST radar and radiosonde observations of inertia-gravity wave climatology over tropical stations: Source mechanisms. *Journal of Geophysical Research: Atmospheres*, *113*(D7), D07109.

Venkat Ratnam, M., Ravindra Babu, S., Das, S. S., Basha, G., Krishnamurthy, B. V., & Venkateswararao, B. (2016). Effect of tropical cyclones on the stratosphere–troposphere exchange observed using satellite observations over the north Indian Ocean. *Atmospheric Chemistry and Physics*, *16*(13), 8581-8591.

Venkat Ratnam, M., Tetzlaff, G., & Jacobi, C. (2004). Global and seasonal variations of stratospheric gravity wave activity deduced from the CHAMP/GPS satellite. *Journal of the Atmospheric Sciences*, *61*(13), 1610-1620.

Vincent, R. A., & Alexander, M. J. (2000). Gravity waves in the tropical lower stratosphere: An observational study of seasonal and interannual variability. *Journal of Geophysical Research: Atmospheres*, 105(D14), 17971-17982.

Vincent, R. A., & Eckermann, S. D. (1990). VHF radar observations of mesoscale motions in the troposphere: Evidence for gravity wave Doppler shifting. *Radio science*, *25*(5), 1019-1037.

Welch, P. (1967). The use of fast Fourier transform for the estimation of power spectra: a method based on time averaging over short, modified periodograms. *IEEE Transactions on audio and electroacoustics*, *15*(2), 70-73.

Wilson, R., Chanin, M. L., & Hauchecorne, A. (1991). Gravity waves in the middle atmosphere observed by Rayleigh lidar: 2. Climatology. *Journal of Geophysical Research: Atmospheres*, *96*(D3), 5169-5183.

Worthington, R. M., & Thomas, L. (1996). The measurement of gravity wave momentum flux in the lower atmosphere using VHF radar. *Radio Science*, *31*(6), 1501-1517.

Wu, D. L., & Waters, J. W. (1996). Satellite observations of atmospheric variances: A possible indication of gravity waves. *Geophysical Research Letters*, *23*(24), 3631-3634.

Zhang, F., Shi, X. F., & Zhang, X. Z. 2009. Study and Simulation of Welch Power Spectrum Estimation Method [J]. *Journal of Xi'an Technological University*, 4: 013.

Table1

Total Number of Occultations before during and after the Five Tropical Cyclones over the Region 4°-45° N and Of 65°-100° E are shown. Average numbers of occultations in each grid of $8^o x 8^o$ are also given.

Cyclone names	Total Occultation over the latitude range of 4°-45° N and longitude range of 65°-100°			Average number of occultation within the grid of 8^ox8^o		
	Before cyclone	During cyclone	After cyclone	Before cyclone	During cyclone	After cyclone
Sidr	438	235	325	20	11	15
Nargis	558	394	503	25	18	23
Aila	422	427	443	19	20	20
Giri	179	143	176	8	7	8
Phailin	293	351	459	13	16	21

Table 2

Different Features Observed During the Five Tropical Cyclones.

Cyclone names	Cate-gory	Landfall region of the cyclones	Maximum wind speed (km/h)	Minimum of average OLR over cyclone path (W/m^2)	Average energy over the cyclone path (J/kg)			Average dominant wavelength over cyclone path (km)		
					Before cyclone	During cyclone	After cyclone	Before cyclone	During cyclone	After cyclone
Sidr	4	Bangladesh	250	171.0	1.94	2.34	1.23	2.41	2.48	2.35
Nargis	4	Border region of Myanmar and Thailand	215	125.0	2.32	3.10	1.16	2.28	2.48	2.41
Aila	1	West Bengal, India and Bangladesh	120	115.6	2.33	2.52	1.64	2.23	2.35	2.17
Giri	4	Myanmar	250	156.8	2.23	3.24	0.94	1.97	2.25	2.21
Phailin	5	Odisha, India	260	160.7	2.37	3.01	1.48	2.17	2.45	2.23

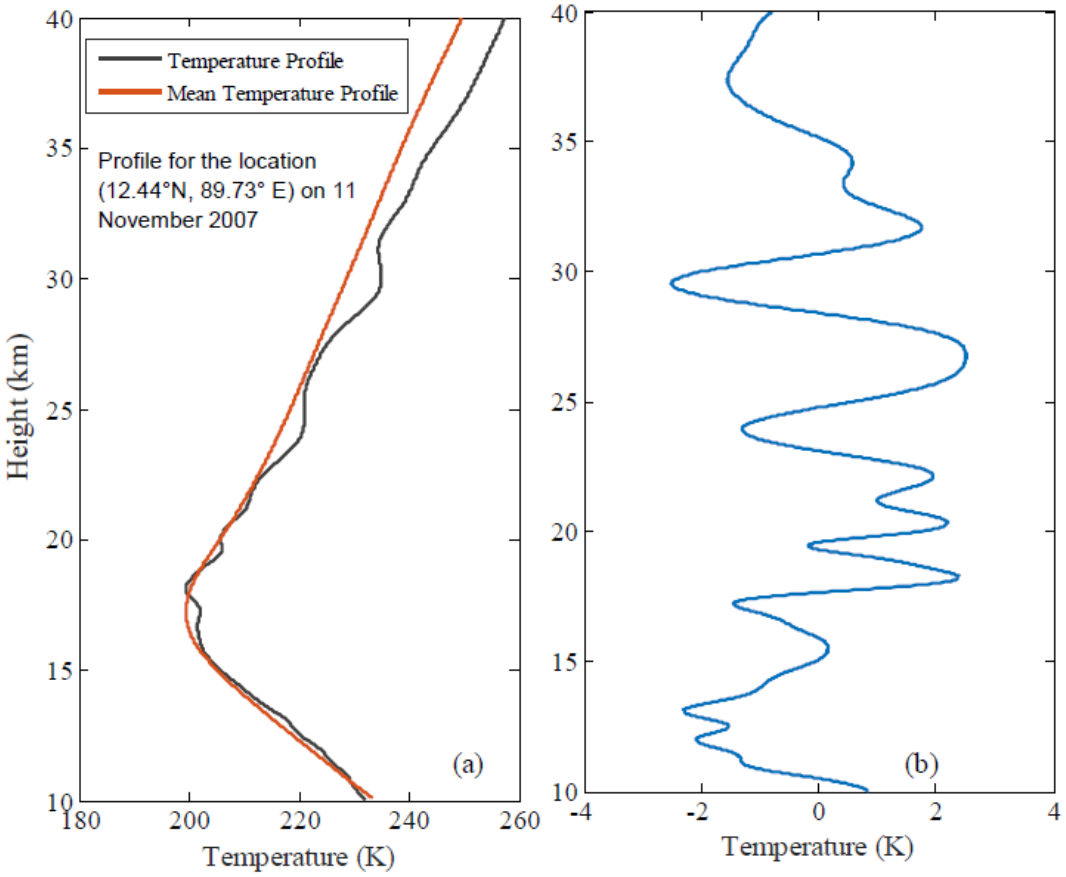

Figure 1. (a) Actual temperature and mean temperature profile and (b) Perturbation profile during the tropical cyclone Sidr for the location (12.44°N, 89.73° E) on 11 November 2007.

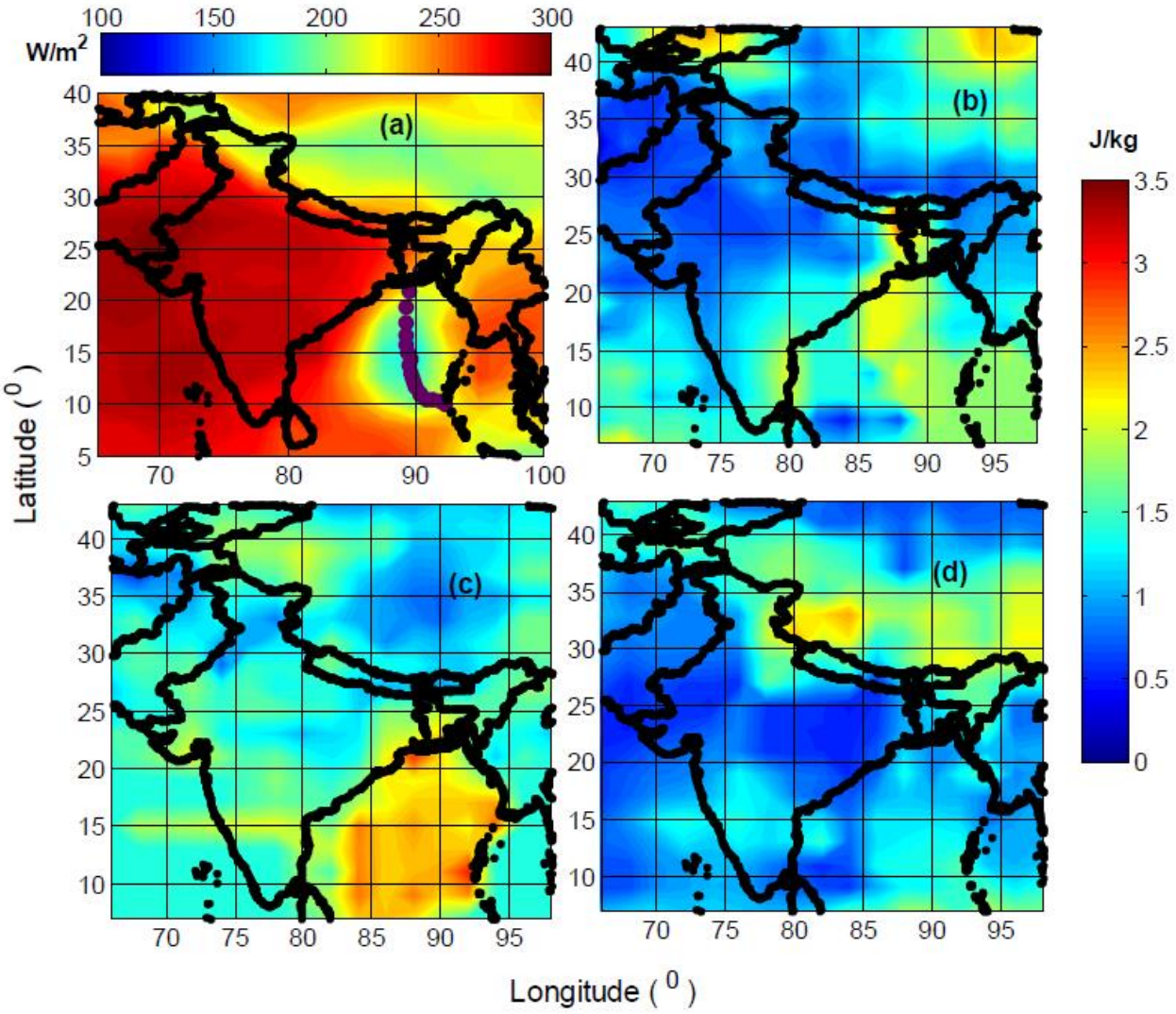

Figure 2. (a) Path of the cyclone Sidr, depicted by filled circles superimposed on the contour plot of average OLR (W/m2) value during 11-16 November 2007. Contour plots of average potential energy (J/kg) in the height range 19-26 km: (b) before the cyclone (3-10 November), (c) during the cyclone (11-16 November), and (d) after the cyclone Sidr (22-29 November 2007).

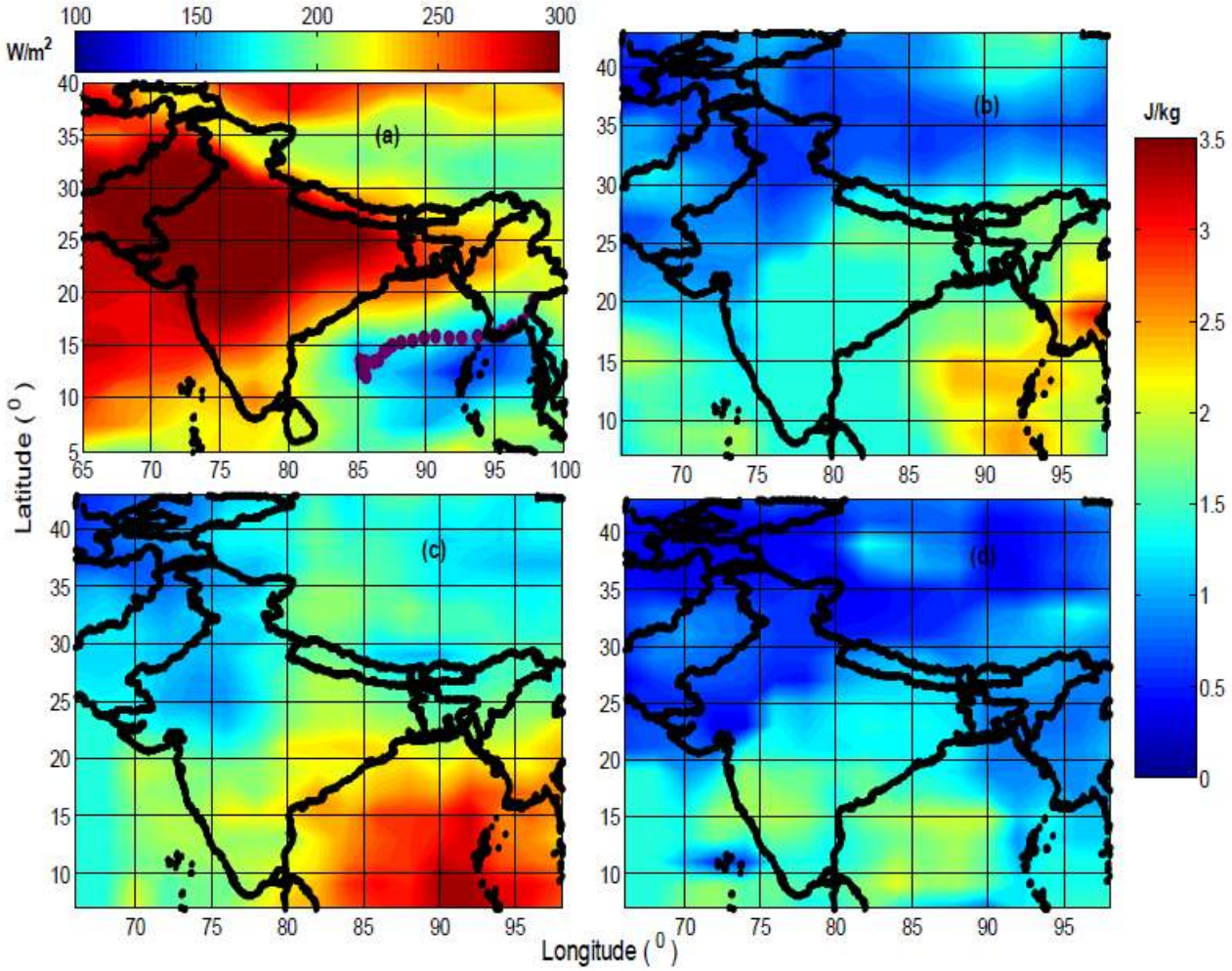

Figure 3. (a) Path of the cyclone Nargis, depicted by filled circles superimposed on the contour plot of average OLR (W/m^2) value **during 27 April-03 May 2008.** Contour plots of average potential energy (J/kg) in the height range 19-26 km: (b) before the storm (18-26 April), (c) during the storm (27 April -03 May), and (d) after the storm Nargis (8-16 May 2008).

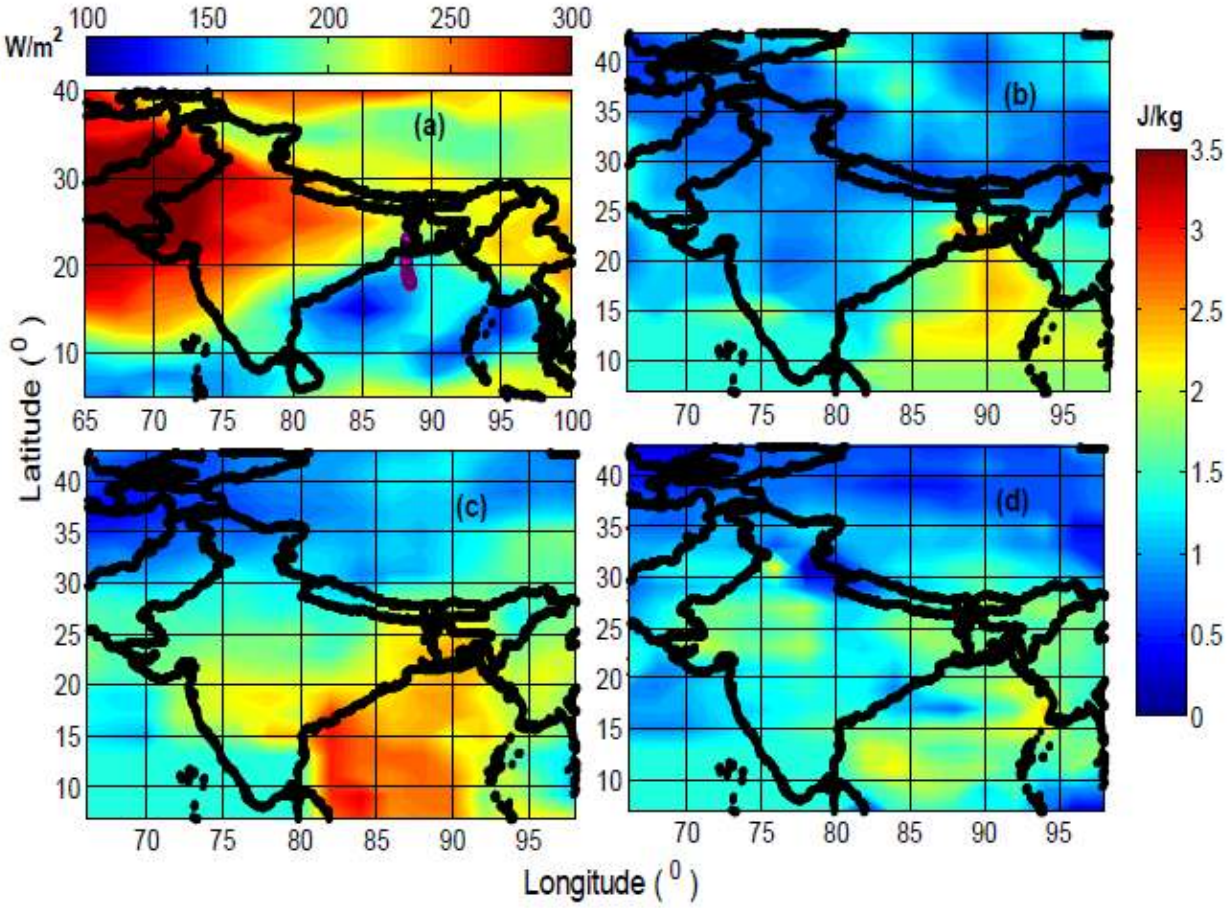

Figure 4. (a) Path of the cyclone Aila, depicted by filled circles superimposed on the contour plot of average OLR (W/m^2) value during 22-27 May 2009. Contour plots of average potential energy (J/kg) in the height range 19-26 km: (b) before the cyclone (15-21 May), (c) during the cyclone (22-27 May), and (d) after the cyclone Aila (2-10 June 2009).

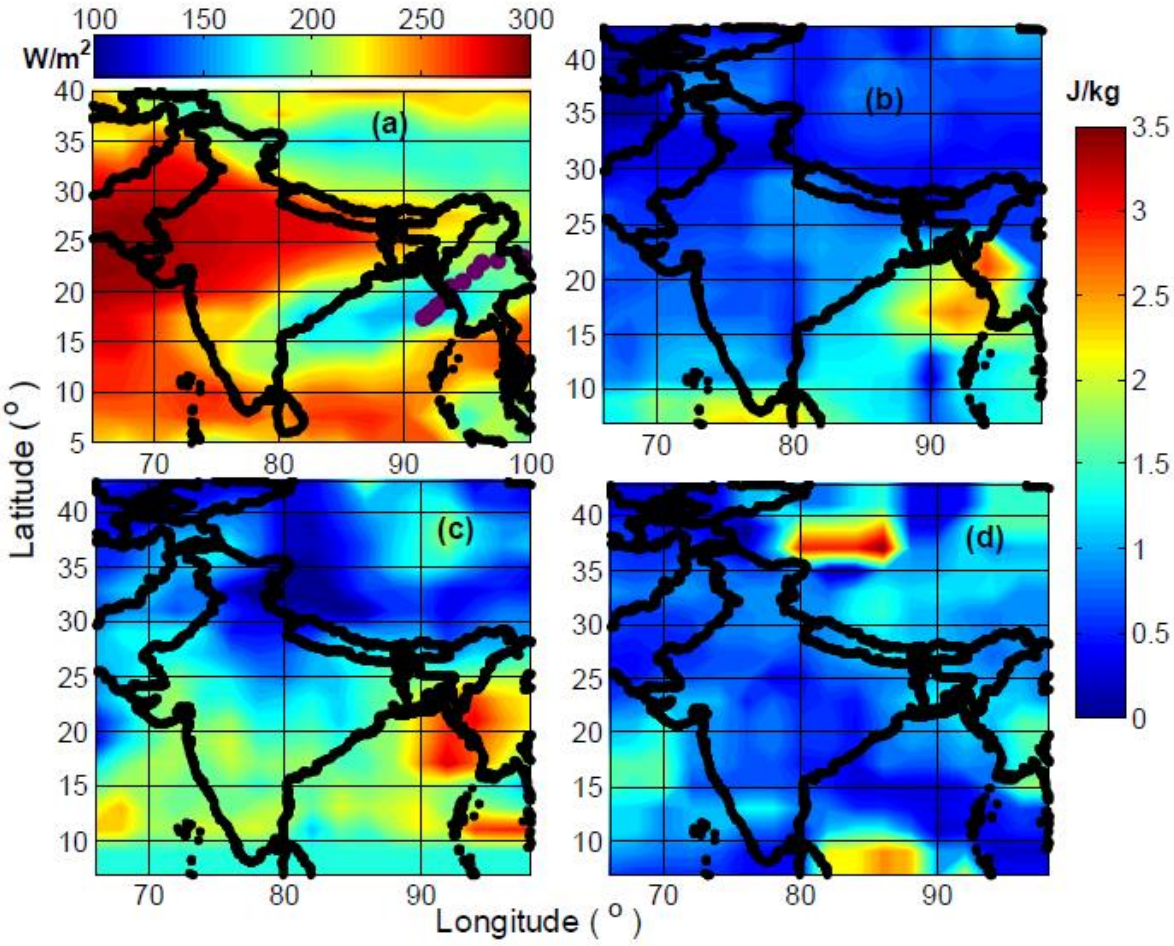

Figure 5. (a) Path of the cyclone Giri depicted by filled circles superimposed on the contour plot of average OLR (W/m^2) value during 20-23 October 2010. Contour plots of average potential energy (J/kg) in the height range 19-26 km: (b) before the cyclone (15 -19 October), (c) during the cyclone (20-23 October), and (d) after the cyclone Giri (28 October - 4 November 2010).

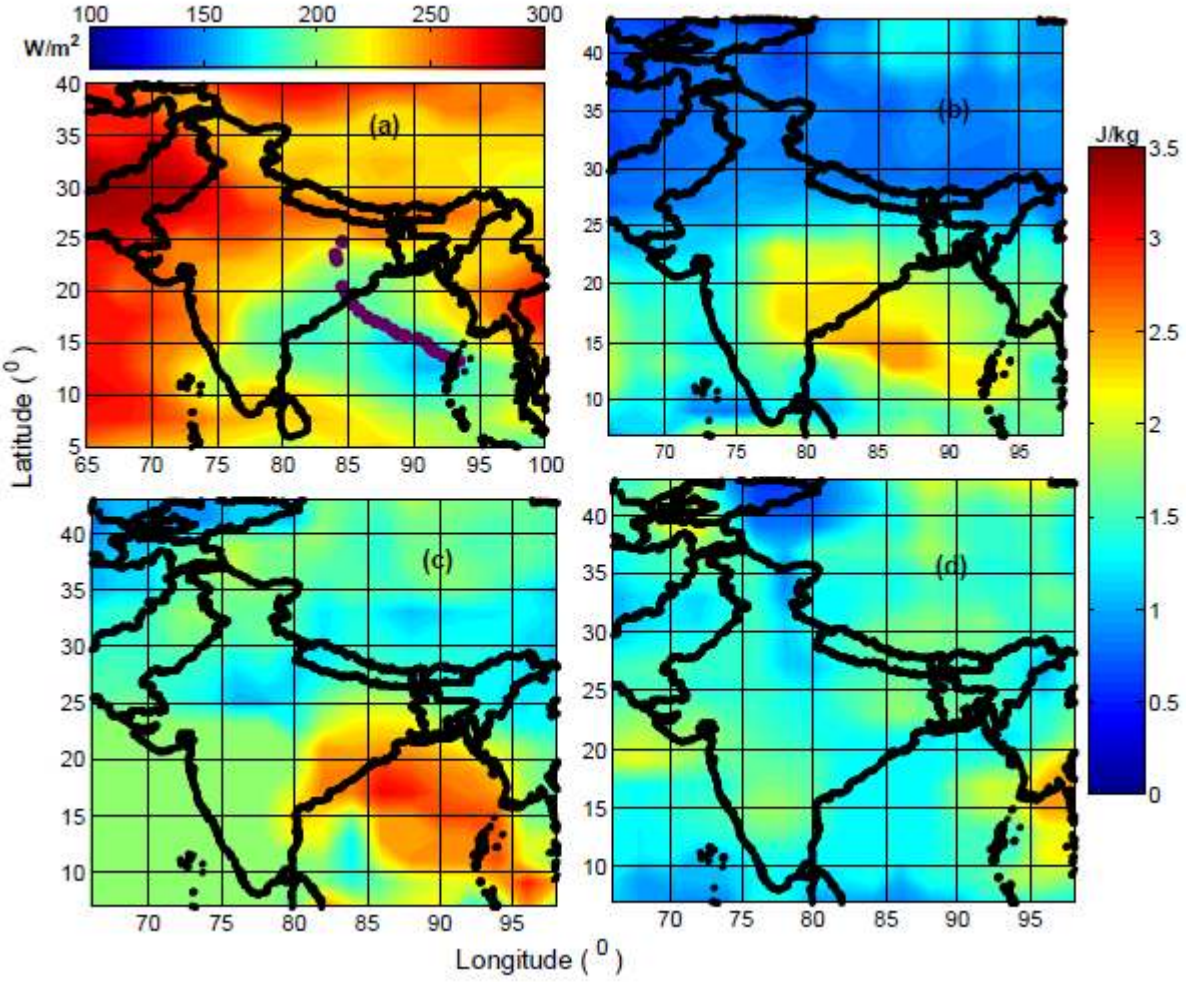

Figure 6. (a) Path of the cyclone Phailin , depicted by filled circles superimposed on the contour plot of average OLR (W/m^2) value during 4-14 October 2013. Contour plots of average potential energy (J/kg) in the height range 19-26 km: (b) before the cyclone (27 September -3 October), (c) during the cyclone (4-14 October), and (d) after the cyclone Phailin (20-28 October 2013).

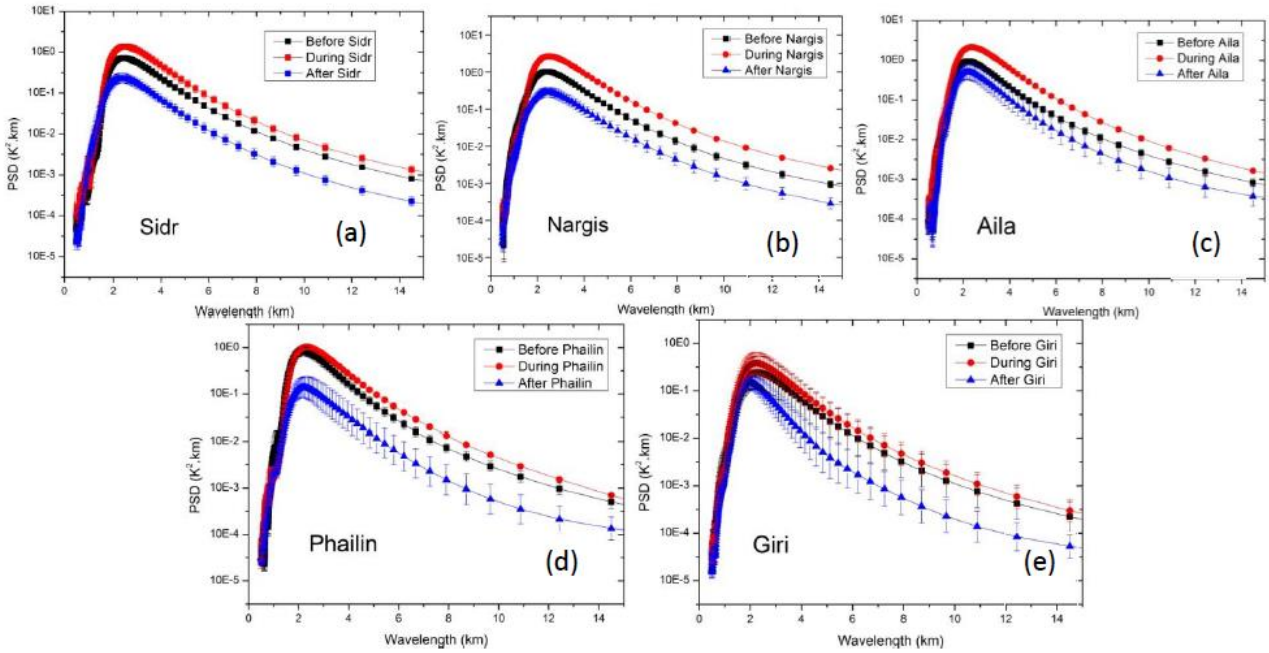

Figure 7. The average power spectral density of gravity wave before, during and after the five cyclones (a) Sidr, (b) Nargis, (c) Aila, (d) Giri, and (e) Phailin.